应用 L-J(12/6)势能模型对 Fe^{2+}水化作用的分子动力学模拟

宋玉财[1] 张志刚[2] 胡文瑄*,[1] 段振豪[2]
([1]南京大学内生金属矿床成矿机制研究国家重点实验室,南京大学地球科学系,南京 210093)
([2]中科院地质与地球物理研究所,北京 100029)

摘要: 本文首先优化出 Fe^{2+}和水分子相互作用的 Lennard-Jones(12/6)势能模型中的 2 个参数:ε_{IW}=0.180 kcal·mol^{-1} 和 σ_{IW}=0.2885 nm。然后在 298.15 K 和 573 K 温度条件下,用这个势能模型去运行 Fe^{2+}极稀水溶液系统的分子动力学模拟。模拟的结果显示,Fe^{2+}的第一和第二水化壳层的结构和动力学性质与实验的, 以及其他势能模型模拟出的结果一致。模拟的同时获得了关于 RWK2 水分子模型内部结构变化的新信息。此外,模拟揭示了温度变化对 Fe^{2+}水化结构和动力学性质的影响。

关键词: L-J(12/6) 势能模型; 参数; Fe^{2+}; 水化性质
中图分类号: P611.1+3; O614.81+1 **文献标识码**: A **文章编号**: 1001-4861(2007)04-0602-09

Molecular Dynamics Simulation of Fe^{2+} Hydration Process using the L-J(12/6) Interaction Potential Model

SONG Yu-Cai[1] ZHANG Zhi-Gang[2] HU Wen-Xuan*,[1] DUAN Zhen-Hao[2]
([1]*State Key Laboratory for Mineral Deposit Reserach, Department of Earth Sciences, Nanjing University, Nanjing* 210093)
([2]*Institute of Geology and Geophysics, Chinese Academy of Sciences, Beijing* 100029)

Abstract: This study initially obtained the two parameters ε_{IW}=0.180 kcal·mol^{-1} and σ_{IW}=0.288 5 nm of the Lennard-Jones (12/6) potential for Fe^{2+}-waters interaction. Then, the L-J (12/6) potential with the two parameters obtained was employed to carry out MD simulation of Fe^{2+} hydration process for a dilute aqueous solution system at 298.15 K and 573 K, respectively. The results show that structural and dynamics properties of Fe^{2+} hydration in the first and second hydration shells agree well with these properties from experiments, as well as other computer simulations in which different Fe^{2+}-waters interaction potentials were employed. Besides, the results give some new insights into RWK2 water intramolecular geometry. In addition, it is also indicated that increasing temperature has a certain impact on the Fe^{2+} hydration structure and dynamics properties.

Key words: L-J(12/6) potential model; parameters; Fe^{2+}; hydration properties

0 Introduction

Fe is one of the most important elements in natural environments and it is involved in a lot of natural processes, either chemically or bio-chemically. In general, the processes take place in H_2O-bearing surroundings, and Fe mostly acts in a Fe^{2+} hydration form. Therefor, the knowledge of Fe^{2+} hydration process is essential to understand the mechanism related to Fe^{2+}-involved reactions. As it is very difficult to perform such a kind of experiment, molecular dynamics (MD) computer simulation method has become a powerful tool of studying ionic hydration process. MD simulation not only can obtain thermodynamic data under extreme *T-P*

收稿日期:2006-10-19。收修改稿日期:2006-12-26。
国家自然科学基金资助项目(No.40673040)。
*通讯联系人。E-mail:Huwx@nju.edu.cn
第一作者:宋玉财,男,28 岁,博士研究生;研究方向:流体地球化学。

conditions, but also can provide fundamental and detailed information about the structure and dynamics of ionic aqueous solution system. However, the success of MD simulation (and Monte Carlo simulation) of ionic hydration process strongly depends on ion-waters interaction potential[1]. Consequently, the application of different potential models to computer simulation is one of common activities in this field.

In previous literatores, several potential models were applied to the MD or MC simulations of Fe^{2+} hydration process that is essential to understand the detailed mechanisms of many chemical, biological and oreforming processes [2,3]. These models include an empirical pair potential[4~9], an *ab initio* effective pair potential[10] and a pair potential plus 3-body correction functions terms model[2]. Comparatively, they are more complicated than the Lennard-Jones (12/6) potential model (L-J). The latter possesses only two adjustable parameters. Due to its simplification and efficiency, the L-J (12/6) potential appears to be the most frequently used to describe ion-waters interaction[11,12]. These ions incl-ude Na^{+}[13], Li^{+}[14], alkali metal ions and alkaline earth metal ions[15], Zn^{2+}[16], Eu^{3+}[17,18], and Nd^{3+}[18]. However, the potential model has not been employed to describe the interaction between Fe^{2+} and waters.

This study attempts to employ the L-J (12/6) potential to perform the MD simulation of Fe^{2+} hydration process. Initially, the two parameters of the L-J (12/6) interaction potential between Fe^{2+} and waters will be optimized. Then, MD simulation for the system of single Fe^{2+} ion and 230 RWK2 water molecules is performed to investigate the ionic structural and dynamical hydration properties, and RWK2 water intramolecular geometry. These results will be compared with experimental and some previous computer simulated results. The simulation is carried out at the temperatures of 298.15 K and 573 K in order to evaluate the impact of temperature on the ion hydration behaviors.

1 Details of calculation

1.1 Interaction potentials and parameters

For a dilute aqueous solution system, interaction potentials include water-water, ion-water and ion-ion. Since our objective is to find out the single ion hydration behavior, the ion-ion interactions will not be discussed here.

The water-water interaction was described using the flexible RWK2 water potential model. The model can yield remarkably good predictions of steam, liquid water, ice, and liquid-vapor phase equilibrium but receives much less attention to date[14]. Its parameters may refer to the Appendix of Duan′s paper (1995)[19].

The ion-water interaction can be expressed:

$$u_{IW}=u_{IW}^{Coulom}+u_{IW}^{Short} \quad (1)$$

Where "I" denotes an ion, "W" stands for a water molecule, u_{IW}^{Coulom} represents the Coulombic interaction and u_{IW}^{Short} is the short-range interaction. In the Coulombic interaction, the partial charges for oxygen and hydrogen atoms are: $2q_H=-q_O=1.2$, which are consistent with the RWK2 water potential model. The pairwise potential function for the short-range interaction was modeled as the Lennard-Jones form:

$$u_{IW}^{Short}=u_{IW}^{LJ}(r_{IW})=4\varepsilon_{IW}\left[\left(\frac{\sigma_{IW}}{r_{IW}}\right)^{12}-\left(\frac{\sigma_{IW}}{r_{IW}}\right)^{6}\right] \quad (2)$$

Where r_{IW} is the distance between the center of the ion and the partial negative charge of the water molecule (its position can be found on the bisector of the H-O-H angle), ε_{IW} and σ_{IW} are the energy and size parameters, respectively.

Based on MD simulated annealing and the steepest descent method[20], the minimum energy structures of $Fe^{2+}(H_2O)_n$ (n=1,2,……) clusters can be calculated. However, because the experimental data of the minimum energy structures of $Fe^{2+}(H_2O)_n$ clusters are scarce at 298.15 K, it is impossible to obtained the two parameters only by best reproducing the binding energy of one ion associated with two or three-water molecule clusters. Therefore, it had to attempt initial estimates of the parameters ε_{IW} and σ_{IW} by fitting the $Fe^{2+}(H_2O)_n$ clusters (n=1, 2, 3, 6) data[21]. Then, the initial parameters were adjusted to improve the agreement of MD simulation with experimentally observed Fe^{2+}-O distances and coordination numbers in the first hydration shell. Consequently, based on the trial procedure, the parameters ε_{IW} and σ_{IW} for Fe^{2+}-water interaction were determined. They are listed in Table 1.

Table 1 Optimized two L-J (12/6) potential parameters for Fe^{2+} ion and water interaction

Interaction	ε_{IW} / (kcal·mol^{-1})	σ_{IW} / nm
Fe^{2+}-H_2O	0.180	0.288 5

1.2 Molecular dynamics simulation

Once the two parameters of the L-J (12/6) potential of Fe^{2+}-water interaction were determined, the potential was employed to perform the NVT canonical ensemble MD simulation for the system of 1 Fe^{2+} ion and 230 RWK2 water molecules. The ion was placed in the cubic box with length of 1.903 nm equivalent to a volume of 18.0 cm^3·mol^{-1}. The periodic boundary conditions and minimum image conventions [11] were used to treat out-of-box atoms and to calculate interatom distances. Long-rang electrostatic forces and energies were calculated using the Ewald sum. In all runs, the time step was set as 31.25 a.u. or 0.75 fs. Initial configurations were selected from the final configurations of previous simulations. Each simulation began with 40 000 steps pre-equilibrium runs followed by 60 000 subsequent steps for data collection. The trajectories of particles were calculated using the Verlet algorithm[22] and the intermediate configurations were saved at certain intervals. Through the analysis of the trajectory configurations as a function of time, the ion hydration properties can be obtained. The calculations above were realized using a FORTRAN code under the software of Visual FORTRAN 65.

The simulation was performed under the temperatures of 298.15 K and 573 K in order to evaluate the impact of temperature on the ion hydration properties. To be pointed out, it is unclear for the quantitative correlation between the L-J (12/6) parameters and temperatures. Here, we directly employed the parameters optimized at 298.15 K to carry out the simulation at 573 K. This is similar to what Yang et al. (2002)[23] and Duan et al. (2003)[20] did in their studies, respectively.

2 Results and discussion

2.1 Radial distribution function and coordination number

Radial distribution function (RDF) of the Fe^{2+} ion-oxygen $g_{IO}(r)$ with coordination number n_O and the RDF of the Fe^{2+} ion-hydrogen $g_{IH}(r)$ with coordination number n_H are described in Fig.1. It is remarkable that two hydration shells are sketched out for $g_{IO}(r)$ and $g_{IH}(r)$, respectively.

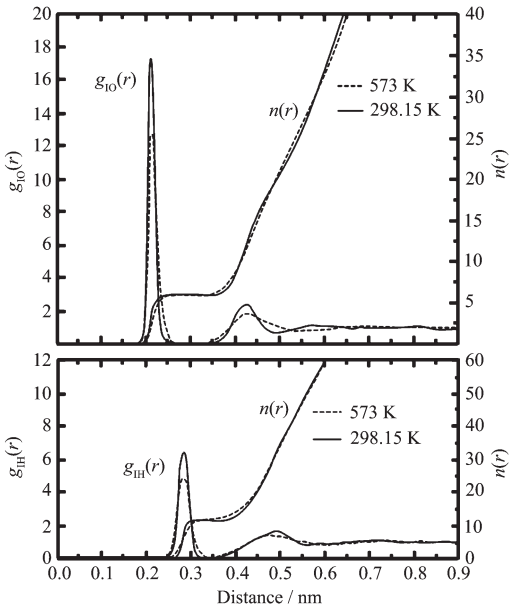

Fig.1 Radial distribution functions of Fe^{2+}-O and Fe^{2+}-H at 298.15 K and 573 K

Table 2 lists the structural properties of the first and second shells from this work, previous experiments and computer simulations. At 298.15 K, our work suggests that R_{IO} is 0.210 nm for the first shell, and is between 0.417 nm and 0.427 nm for the second shell. R_{IH} is 0.283 nm for the first shell, and 0.490 nm for the second shell. Correspondingly, the coordination number n_O is 6.0 in the first shell, and 13.0 in the second shell. NH is 12.0 in the first shell. Our results are in good agreement with the results from the previous experiments and simulations (Table 2).

Those the effect of temperature on the RDF of ion-oxygen and ion-hydrogen and the coordination number can be evaluated. Fig.1 shows that with the temperature increasing from 295.15 K to 573 K, the peak positions of the first and second hydration shells do not shift. Also, the coordination number n_O and n_H in the first shell are almost unchanged, indicating that the shell is quite stable to avoid the entrance of more water molecules. However, the coordination number n_O in the second shell increased by 5 ± 1 and n_H increased by 11.5 ± 2 (Table 2). This implies that

Table 2　Structural properties for Fe^{2+}-water in hydration shells[a]

Characteristics[b]	Method / Reference[c]	First hydration shell	Second hydration shell
R_{IO} / nm	MD / This work	0.210	0.417~0.427
	MD / This work	0.210 (at 573 K)	0.424 ± 0.006 (at 573 K)
	EX / [6,24]	0.210, 0.218	
	X / [25]	0.212	
	N / [25]	0.213	
	EX, N, X / [26]	0.210~0.228	0.430~0.451
	X, EX / [27]	0.210	
	MD / [4,5,7,8]	0.211, 0.215, 0.195, 0.2075	
	MC / [9]	0.210	0.421
R_{IH} / nm	MD / This work	0.283	0.490
	MD / This work	0.278 (at 573 K)	0.481 ± 0.006 (at 573 K)
	N / [26]	0.275	
	MD / [5,8]	0.289, 0.277 5	
	MC / [9]	0.278	
n_O	MD / This work	6.0	13.0
	MD / This work	6.0 (at 573 K)	18 ± 1 (at 573 K)
	EX / [6,24]	6, 6	
	X / [25]	6	
	N / [25,26]	6, 6	
	QM-MM / [24]	6	12.4
	EX, N, X / [26]	5.1–6.1	
	X, EX / [27]	6	
	MD / [4,5,7,8]	6, 6, 6, 6	
	MC / [9]	6	12.96±1.44
n_H	MD / This work	12.0	36.5
	MD / This work	12.1 (at 573 K)	48±2 (at 573 K)
	N / [26]	12.1	
	MD / [7]	12	
	MC / [9]	12	
θ	MD / This work	168°	130.3°
	MD / [8]	163°	
	MC / [9]	162°	
∠HOH	MD / This work	103.51	104.60
	QM-MM / [25]	104.7	100.8
	MD / [8]	105.7	
$R_{O\text{-}H}$ / nm	MD / This work	0.099 0	0.098 0
	QM-MM / [24]	0.096	0.097 2
	MD / [8]	0.101 8	

Note: [a] Except the data marked by 'at 573 K', the other data were determined at the temperatures of near 298.15 K. [b] R_{IO} and R_{IH} denote the peak positions of Fe^{2+}-O and Fe^{2+}-H RDF distribution, respectively. [c] EX, Extended X-ray absorption fine structure; X, X-Ray Diffraction; N, Neutron Diffraction; MD, Molecular Dynamics simulation; MC, Monte Carlo simulation; QM/MM, combined quantum mechanical/molecular mechanical molecular dynamics simulation.

when temperature increases, water molecules are easy to overcome the energy barrier to enter into the second shell, and the shell becomes strikingly less stable.

2.2　Orientation of water molecules in hydration shells

Although RDF can provide the fundamental

structural information, in order to elucidate a three-dimensional structural image, it is useful to describe orientations of water molecules in hydrations. Herein, the dipole-ion angle (θ) distribution and the O-ion-O angle distribution are investigated.

Fig.2 shows that the distributions of θ values in the first shell and second hydration shell. At 298.15 K, the distribution peak of θ values in the first shell is located at around 168° (Table 2). In general, the value is similar to the values reported in previous simulations. Those simulations suggest that Fe^{2+} more stably lays 160°~170° away from the H-O-H bisector in the first shell (Table. 2). The distribution peak of θ values in the second shell is located at around 130° (Table 2), with larger fluctuations than that in the first shell (Fig.2). It implies that the ionic repulsion on the dipole decreases with increasing distance away from the Fe^{2+} ion.

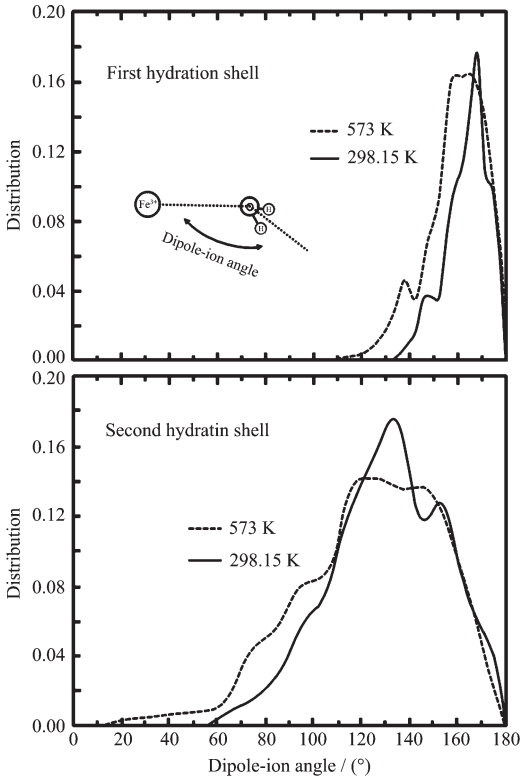

Fig.2 Distributions of dipole-ion angle in the first hydration shell, and in the second hydration shell at 298.15 K and 573 K

When the temperature increased to 573 K, the distribution peak of θ values turns to be broadened and lower whatever for the first shell or the second shell (Fig.2). Meanwhile, the peak positions shift towards narrower θ value. This means that increasing temperature reduces the angle of the H-O-H bisector opposite to the ion-O direction.

Fig.3 gives the O-ion-O angle distributions in the first shell and the second shell. There are two pronounced peaks in the first shell at 298.15 K: the first one is centered on 90° and the second one is centered on around 180° (Fig.3). The characteristics clearly demonstrate a regular octahedron of water molecules of the first shell around the Fe^{2+} ion, which is consistent with previous results[2,8,9,24]. In the second shell, two tallish peaks centered on about 66° and about 109° are found, but their fluctuations are so larger that it is impossible to figure out its spatial structure (Fig.3).

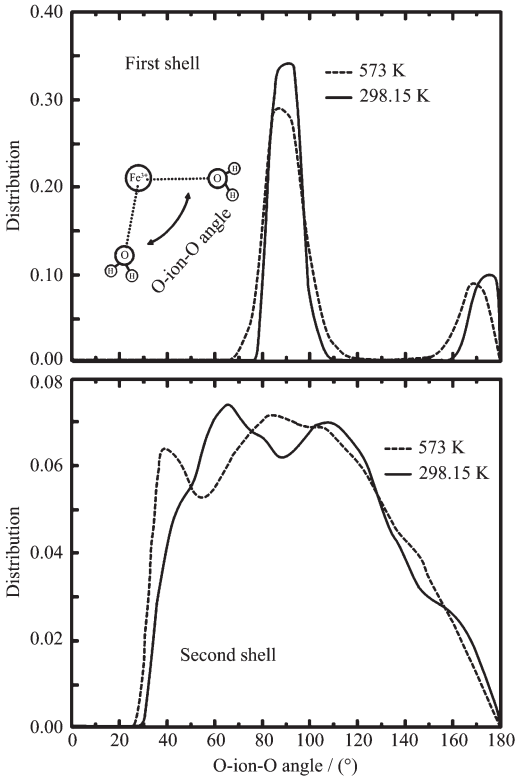

Fig.3 Distributions of O-Fe^{2+}-O angle in the first hydration shell, and in the second hydration shell at 298.15 K and 573 K

With increasing temperature to 573 K, both peaks of O-ion-O angles in the first shell decrease by about 10°. It indicates that increasing temperature may slightly distort the stable octahedron structure of the ion-water in the first shell, but still not enough to

destroy it. The O-ion-O angle distribution in the second shell is also changed, implying that temperature has a certain impact on the structure of the hydration shell.

2.3 Hydrogen bonding analysis

A geometric criteria is taken to identify the formation of hydrogen bonds: if the oxygen atom of a water molecule A is within the distance of 0.35 nm of the oxygen atom of another water molecule B, and the H (of A)⋯O–H (of B) angle is greater than 140°, a hydrogen bond is assigned [28,29]. The oxygen atom of water molecules B will be counted as an "acceptor" and the oxygen atom of water molecules A will be counted as a "donator".

Initially, the average acceptors and donators per molecules in pure water were calculated. The result shows that they have the same value of 1.745 at 298.15 K, and 1.309 at 573 K. Subsequently, the average number of acceptors and donators of hydrogen bonds per water molecules in the ionic aqueous solutions were calculated. Table 3 lists their values with variable distances from the ferrous ion. At 298.15 K, within the distance of around 0.4 nm from the Fe^{2+} ion, the distance is shorter, and the average acceptors are fewer while the average donators keep comparatively stable numbers (a little more than 1.745 of pure water). Out of the distance, the acceptors and donators numbers keep comparatively stable, approximately equal to 1.745. Summing the number of average acceptors and corresponding donators, we can get the average number of hydrogen bonds per water molecules. Fig.4 displays that the average number of hydrogen bonds per water molecules with variable distances from the ferrous ion. The horizontal line represents the average number of hydrogen bonds per molecule in pure water. It is clear that within around 0.4 nm, the solid curve is distinctly lower than the horizontal solid line. However, out of around 0.4 nm, the solid curve is approximately close the horizontal solid line. Therefore, we may consider that in the vicinity of a cation where is not in favor of formation of "hydrogen bonds". Out of a certain distance, the ion has almost negligible effects on the hydrogen bonds of water molecules.

Table 3　Average numbers of acceptor and donator of hydrogen bonds per water molecule with variable distances from Fe^{2+} ion

Distance / nm	Number (298.15 K)		Number (573 K)	
	Acceptor	Donator	Acceptor	Donator
0~0.2	0	1.812	0	1.658
0.2~0.3	0.007	1.855	0.044	1.499
0.3~0.4	1.372	1.767	0.921	1.337
0.4~0.5	1.684	1.744	1.307	1.326
0.5~0.6	1.775	1.753	1.302	1.304
0.6~0.7	1.825	1.761	1.373	1.306
0.7~0.8	1.779	1.735	1.333	1.286
0.8~0.9	1.819	1.747	1.359	1.305

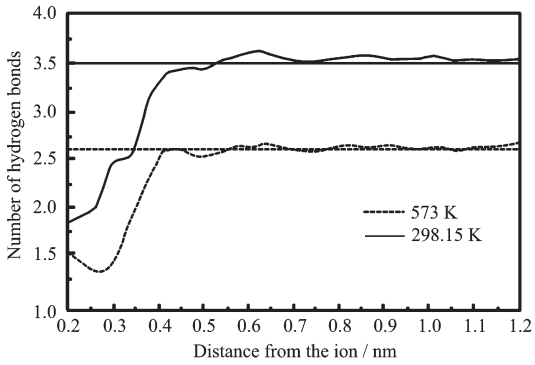

Horizontal lines represent the values of pure water system

Fig.4　Average number of hydrogen bonds per water molecules for the hydration system with variable distances from the ion at 298.15 K and 573 K

When temperature increased from 298.15 K to 573 K, the average acceptors and donators of hydrogen bonds per water molecule significantly decrease (Table 3). This situation is generally indiscriminated for the vicinity of the ion or the region far from the ion, although the exception exists for the distance of 0.2 nm to 0.3 nm from the ion. As far as pure water, its average acceptors and donators are reduced from 1.745 to 1.309. Equally, the average hydrogen bonds per water molecule also decreased. It can be seen from Fig.4 that the dash line is always below the solid line.

With increasing temperature from 298.15 K to 573 K, the number of hydrogen bonds decreases. The simulation gives the correct number of hydrogen bonds for pure water at 3.490 at 298.15 K. It is unclear whether the value of 2.618 at 573 K is correct or not,

because the corresponding value cant be found in previous literatures. However, it is certain that increasing temperature plays a negative role in formation of hydrogen bonds. This can also be proved by lifetimes of hydration bonds. The simulation shows that the longest lifetime of hydration bonds is around 19.5 ps and the average lifetime is 1.20 ps at 298.15 K. Whereas, when the temperature is 573 K, the longest lifetime is less than 3.0 ps and the average lifetime is around 0.28 ps.

2.4 Dynamical residence time

Previous experimental results indicate that the dynamical residence time of water molecule in the first hydration shell of Fe^{2+} is 10^{-6}~10^{-7}s at 298.15 K[26], meaning that the time is several orders of magnitude longer than our simulation time. Accordingly, no water molecule exchange process is observed in the first hydration shell during our 45 ps simulation. However, water molecule exchange process can be found in the second hydration shell during the simulation time. The longest residence time of water molecules in the shell is around 13 ps, approximately equal to a 10 ps of the mean residence time determined by a MD simulation[3].

An attempt is made to analyze the residence time of water molecules in the second hydration shell at 573 K. Our calculation shows the longest residence time of water molecules in the second hydration shell is only several picoseconds. It indicates that with the increasing of temperature, the residence time distinctly decreases. The observation should be reasonable[23].

2.5 Intramolecular geometry of RWK2 water

For the analysis of the RWK2 water intramolecular geometry, the distributions of H-O-H angles (∠H-O-H) and O-H distances ($R_{O\text{-}H}$) of water molecu-

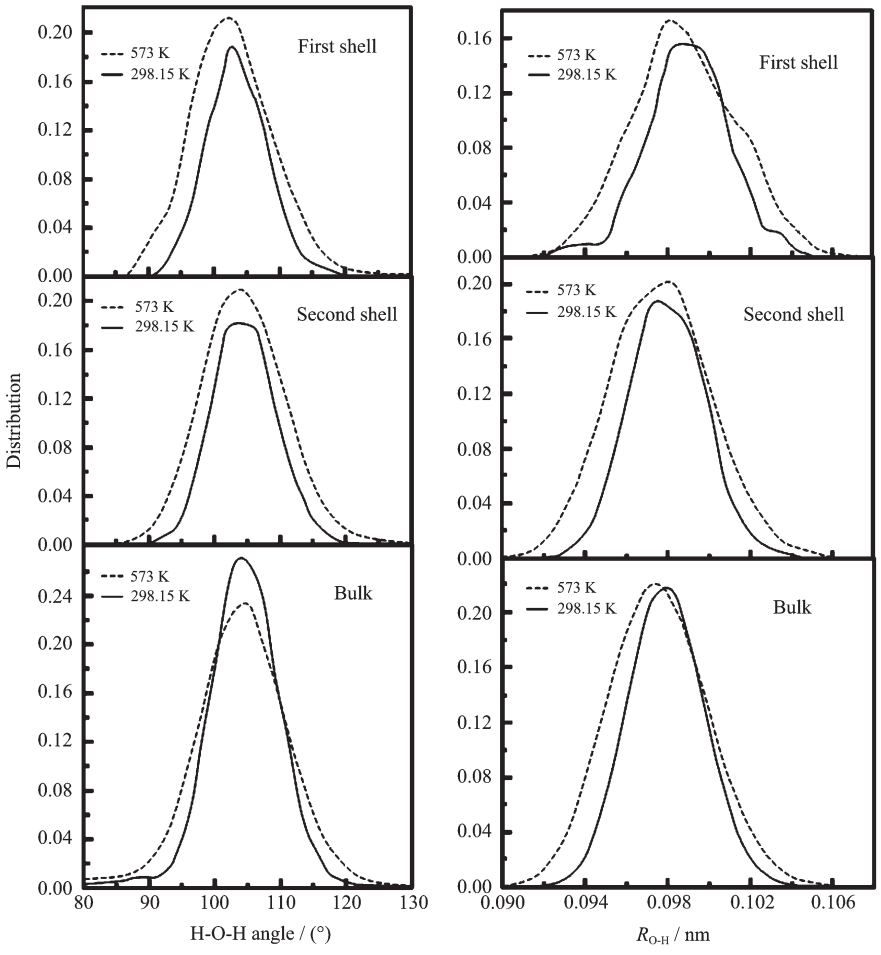

Fig.5 Distributions of H-O-H angle and O-H distance of water molecules in the first hydration shell, in the second hydration shell, and in the bulk at 298.15 K and 573 K

les were investigated. The distributions are described in Fig.5 and their average values are listed in Table 2.

At 298.15 K, the peak of ∠H-O-H distribution in the first shell is located at the left of that in the second shell or in the bulk (Fig.5). It denotes that the ∠H-O-H is generally narrower in the first shell than that in the second shell or in the bulk. The peak of $R_{O\text{-}H}$ distribution in the first shell is located at the right of that in the second shell or in the bulk. It means that the $R_{O\text{-}H}$ is longer in the first shell than that in the second shell or in the bulk. Generally, the intramolecular geometry of water in the second shell and the bulk are indistinguishable. Table 2 shows that their average ∠H-O-H values are around 104.60° and their average $R_{O\text{-}H}$ values are around 0.098 0 nm. These values agree well with the results from a MD simulation [19] that was carried out for the system of pure RWK2 water. The characteristics of the intramolecular geometry show that within the region of the first shell, the ferrous ion has stronger influence on the geometry of the RWK2 water intramolecule. Whereas, once departing from the region, the influence turns to be weaker, and the geometry is near to that of pure water.

In previous simulations of Fe^{2+} hydration, BJH-CF2 water gave 104.7° of the average ∠H-O-H in the first shell and 100.80° of that in the second shell (Table 2). A central force water model gave 105.7° of that in the first and second shells. Obviously, they have larger the H-O-H angle than the RWK2 water. Also, Table 2 shows that BJH-CF2 water has smaller O-H distance of water intramolecule whatever in the first or second shell than the RWK2 water but the central force water model has larger the O-H distance than the RWK2 water.

Fig.5 shows that increasing temperature can enhance the bending of H-O-H and the stretching of O-H of water intramolecule, leading to wider distributions of the ∠H-O-H and $R_{O\text{-}H}$ values. The peaks of the ∠H-O-H distributions in both hydration shells are nearly unchanged, but the peak positions of $R_{O\text{-}H}$ distributions will shift towards the shorter or longer $R_{O\text{-}H}$ value. It seems that temperature has stronger impact on the O-H distance than on the H-O-H angle of the RWK2 water intramolecule.

3 Summary

This work initially determined the two parameters ε_{IW} =0.180 kcal·mol^{-1} and σ_{IW} =0.2885 nm of the Lennard-Jones (12/6) potential of Fe^{2+}-water interaction. Then, the L-J (12/6) potential and the flexible RWK2 water model were employed to carry out the MD simulation of Fe^{2+} hydration processes for a dilute aqueous solution system. At 298.15 K, (1) the peak position of Fe^{2+}-O radial distribution functions (RDF) is located 0.210 nm for the first hydration shell where 6 water molecules reside, and 0.417~0.427 nm for the second shell where 13 water molecules reside. The peak position of Fe^{2+}H RDF is located 0.283 nm for the first hydration shell that contains 12 hydrogen molecules. (2) Six water molecules in the first shell form a regular octahedron structure and Fe^{2+} stably lays around 168° away from the H-O-H bisector in the shell. (3) Within around 0.4 nm away from the Fe^{2+} ion, the average number of hydrogen bonds per molecule is lower than the number in pure water. However, out of the distance of around 0.4 nm, the average number of hydrogen bonds per molecule has approximately same number with that of pure water. (4) No water molecule exchange process is observed in the first hydration shell during the 45 ps simulation due to the time is too short compared to the 10^{-6}~10^{-7} s residence time of water molecules. However, water molecule exchange process can be found in the second hydration shell where the longest residence time of water molecules is around 13 ps. (5) For the intramolecular geometry of RWK2 water, the H-O-H angle is narrower but the O-H distance is longer in first shell than in second shell or in the bulk. It seems that RWK2 water has different intramolecular geometry with BJH-CF2 water and a central force water model. In general, the structural and dynamics properties by our simulation agree well with experimental and previous computer simulated results. It is reasonable to consider that the L-J (12/6) potential with the determined parameters is available to

describe the Fe^{2+}-waters interaction.

The impact of temperature on Fe^{2+} hydration behaviors is evaluated in this simulation. (1) The increase of temperature lets the statistic distribution peaks of the ionic hydration structural properties turn to be wider and less sharp. The observations are consistent with that increasing temperature can enhance the translational motion and vibration of water molecules. (2) Increasing temperature can result in the increases of the coordination numbers in the second hydration shell but it is not easy to change that in the first shell. (3) Increasing temperatures makes the dipole angle be narrower, and slightly distorts the stable octahedron structure of waters in the first shell. (4) The increases of temperature may reduce the numbers of hydrogen bonds, and decrease the lifetime of hydrogen bonds and the residence time of the water molecules in hydration shells. (5) Increasing temperature shortens or elongates the O-H distances of the RWK2 water intramolecules in hydration shells, but lays less impact on the H-O-H angles.

References:

[1] Yagüe J I, Mohammed A M, Loeffler H H, et al. *Theochem.*, **2003**,**620**:15~20

[2] Barnes H L. *Geochemistry of Hydrothermal Ore Deposit*s, New York: John Wiley and Sons, **1997**.972

[3] Remsungnen T, Roke B M. *Chemical Physics Letters*, **2004**, **385**:491~497

[4] Curtiss L A, Halley J W, Hautman J, et al. *J. Chem. Phys.*, **1987**,**86**:2319~2327

[5] Kuharski R A, Bader J S, Chandler D. *J. Chem. Phys.*, **1988**, **89**:3248~3257

[6] Kneifel C L, Friedman H L, Newton M D. *Z. Naturforsch*, **1989**,**44**:385~394

[7] Kumar P V, Tembe B L. *J. Chem. Phys.*, **1992**,**97**:4356~4367

[8] Guàrdia E, Padró J A. *Chem. Phys.*, **1990**,**144**:353~362

[9] Degrève L, Quintale C. *J. Electroanal. Chem.*, **1996**,**409**:25~31

[10]Floris F, Persico M, Tani A, et al. *Chem. Phys. Letter*, **1992**, **199**:518~524

[11]Allen M P, Tildesley D J. *Computer Simulation of Liquids*. Oxford: Oxford Science Publications, **1987**.385

[12]Nasehzadeh A, Mohseni M, Azizi K. *Theochem.*, **2002**,**589**~**590**:329~335

[13]Driesner T, Seward T M, Tironi I G. *Geochim. Cosmochim. Acta*, **1998**,**62**:3095~3107

[14]Duan Z H, Zhang Z G. *Molecular Physics*, **2003**,**101**:1501~1510

[15]Satheesan B, Carmay L. *J. Phys. Chem. B*, **1999**,**103**:7958~7968

[16]Obst S, Bradaczek H. *J. Mol. Model.*, **1997**,**3**:224~232

[17]Chaussedent S, Monteil A. *J. Chem. Phys.*, **1996**,**105**:6532~6537

[18]Kim H S. *Chem. Phys.*, **2001**,**269**:295~302

[19]Duan Z, Moller N, Weare J H. *Geochim. Cosmochim. Acta*, **1995**,**59**:3273~3283

[20]Leach A R. *Molecular Modeling: Principles and Applications*. Longman: Essex, **1996**.587

[21]Jafri J A, Longan J, Newton M D. *Israel J. Chem.*, **1980**,**19**: 340~350

[22]Enderby J E, Neilson G W. *Water: A Comprehensive Treatise. Vol.*6. Franks F. Ed., New York: Plenum, **1979**.1~46

[23]Yang T, Tsushima S, Suzuki A. *Chem. Phys. Lett.*, **2002**,**360**: 534~542

[24]Remsungnen T, Roke B M. *J. Phys. Chem. A*, **2003**,**107**:2324~2328

[25]Ohtaki H. *Monatshefte Fur Chemie*, **2001**,**132**:1237~1268

[26]Ohtaki H. *Chem. Rev.*, **1993**,**93**:1157~1204

[27]Marcus Y. *Chem. Rev.*, **1988**,**88**:1475~1498

[28]White J A, Schwegler E, Galli G, et al. *J. Chem. Phys.*, **2000**, **113**:4668~4673

[29]Venables D S, Schmuttenmaer C A. *J. Chem. Phys.*, **2000**, **113**:11222~11236